Journal of Power Sources 196 (2011) 8360–8365

Contents lists available at ScienceDirect

Journal of Power Sources

journal homepage: www.elsevier.com/locate/jpowsour

Highly dispersed Pt nanoparticles supported on poly(ionic liquids) derived hollow carbon spheres for methanol oxidation

Xiangjie Bo, Jing Bai, Jian Ju, Liping Guo*

Faculty of Chemistry, Northeast Normal University, Changchun 130024, PR China

ARTICLE INFO

Article history:
Received 16 June 2011
Accepted 20 June 2011
Available online 28 June 2011

Keywords:
Hollow carbon spheres
Platinum
Methanol oxidation
Poly(ionic liquids)

ABSTRACT

Hollow carbon spheres (HCSs) are prepared using poly(ionic liquids) (PILs) as a carbon precursor and monodisperse silica particles as a template for the first time. The ILs form a uniform polymer coating on the template surface after polymerization. Carbonization of the coating and the subsequent removal of the template produces porous carbon spheres with a hollow structure. The HCSs possess a high surface area, good conductivity, and porosity suitable for mass transport, and they can be used as a support for Pt electrocatalysts. Pt nanoparticles with an average size of 2.8 nm are homogeneously distributed onto the HCSs. The high surface area and unique structure facilitates the fine dispersion of Pt nanoparticles. The obtained Pt/HCSs exhibit a significant catalytic activity for the oxidation of methanol.

1. Introduction

Direct methanol fuel cells (DMFCs) have received considerable attention for application as a clean and portable power source due to their high energy density, relatively low operating temperatures, and low emissions. Pt and Pt-based alloys are widely used as electrocatalysts in DMFCs, and a great deal of effort has been devoted to the synthesis of different nanostructured Pt materials with the goal of improving their catalytic activity. Recent reports indicate that the electrocatalytic activity of some platinum-containing bimetallic alloys (transition-metals or rare earth metal) is superior to those of the pure Pt metal [1–3]. Electrocatalytic performance also depends on the structure and morphology of the support material. Carbon materials with a hollow structure, which facilitates ion transport by reducing the resistance and the length of the diffusion pathways, are recommended for the support of the electrocatalysts. The unique structure and excellent properties, including a suitable porosity, high specific surface area, and large pore volume, of hollow carbon spheres (HCSs) have made them a very attractive support for noble metal nanoparticles with high electrocatalytic performance [4–7]. A wide variety of novel methodologies for the preparation of HCSs have been reported, one of which, the hard template method, is a widely employed technique due to its simplicity [4,7–10]. This method can easily control the structural properties of the resulting carbon materials and involves the infiltration of the template with a monomer or polymer precursor and then polymerizing or cross-linking it. Carbonization and the subsequent removal of the template result in a material with pores that were originally occupied by the template species.

Because of their high stability, high electrical conductivity, and low vapor pressure, ionic liquids (ILs) hold great promise for electrochemical applications [11–14]. Dai and co-workers proposed a novel method for the synthesis of porous carbon materials from ILs [15,16]. Dai and Wang reported an attractive strategy for forming functional, porous carbon and carbon-oxide composite materials through the confined pyrolysis of ILs within a silica network [17]. Mesoporous carbon materials were conveniently made by the carbonization of nucleobases dissolved in all-organic ILs and showed a very high catalytic activity for the reduction of oxygen [18]. Recently, ILs were used in the synthesis of ordered mesoporous graphitic carbon using SBA-15 as a template [19]. Compared to carbon materials derived from conventional precursors, those formed from ILs are rather expensive. However, the large number of possible combinations of cations and anions provides a great opportunity to create tailor-made, porous carbon materials from ILs. The structural morphology, porosity, and surface area of the resulting carbon material are strongly dependent on the nature of the cation/anion pairing in the ILs [15,16]. Due to their very low vapor pressure, another application of ILs is as a nonvolatile precursor, which reduces any mass loss before the beginning of the decomposition process [20]. The favorable interaction of the strongly polar ILs with the polar inorganic silica templates facilitates the synthesis of a high surface area, nitrogen-doped carbon with varying morphologies [21]. Nitrogen and other elements can be introduced into the porous carbon structure by employing ILs

* Corresponding author. Tel.: +86 0431 85099762; fax: +86 0413 85099762.
E-mail address: guolp078@nenu.edu.cn (L. Guo).

0378-7753/$ – see front matter © 2011 Elsevier B.V. All rights reserved.
doi:10.1016/j.jpowsour.2011.06.068

that contain the desired heteroatom. However, these reports concerned the direct pyrolysis of the ILs, and it was difficult to control the morphology of the obtained carbon materials due to the fluidic properties of the ILs. Yuan et al. used ILs monomers to form a PILs, and then, the direct carbonization of the PILs was performed in the presence of $FeCl_2$ to obtain the mesoporous graphitic carbon [20]. It was found that $FeCl_2$ played a key role in controlling the chemical structure of the obtained carbon materials, but few works are available on the fabrication of carbon material using PILs as carbon precursors via the hard template method. The PILs can be used to overcome the fluidity of ILs. When a PILs was used as the carbon precursor, the ILs formed a uniform polymer coating on the template surface after polymerization. The morphology of the obtained material can be controlled by manipulating the template structure.

In this work, monodisperse SiO_2 particles were used as the template, and PILs was used as the carbon source. The SiO_2 surface was coated with a uniform PILs layer to create core/shell composite spheres. Carbonization and subsequent removal of the template generates carbon spheres with a hollow structure. The monodisperse silica particles used as the hard template are commercially available or can be obtained through a simple synthesis. To the best of our knowledge, this is the first report of using a PILs as a carbon precursor for the fabrication of HCSs. HCSs possess high surface area, good conductivity, and suitable porosity for mass transport, and they can be used as a suitable support for making Pt electrocatalysts. The obtained HCSs were further used as the support of a Pt catalyst that was compared to a Pt/Vulcan XC-72 catalyst. The Pt/HCSs exhibited a significant catalytic activity for the oxidation of methanol.

2. Experimental

2.1. Reagents and apparatus

Monodisperse SiO_2 spheres with an average diameter of 105 nm were synthesized using the Stöber method [22]. Nafion (5 wt%) was purchased from Sigma–Aldrich. 2,2′-Azobisisobutyronitrile (AIBN), $H_2PtCl_6{\cdot}6H_2O$, formic acid, and methanol were purchased from Sinopharm Chemical Reagent Co., Ltd. China. 1-Vinyl-3-ethylimidazolium tetrafluoroborate ([VEIM]BF_4) was purchased from Lanzhou Greenchem ILS, LICP, CAS, China.

The X-ray diffraction (XRD) pattern was obtained on an X-ray D/max-2200vpc (Rigaku Corporation, Japan) instrument operated at 40 kV and 20 mA using Cu Kα radiation (k = 0.15406 nm). Philips XL-30 ESEM was used to determine the morphology of product. The HCSs were cast on indium tin oxide (ITO)-coated glass for SEM measurement. Transmission electron microscopy (TEM) images were obtained using a JEM-2100F transmission electron microscope (JEOL, Japan) operating at 200 kV. The nitrogen adsorption–desorption isotherm was performed on an ASAP 2020 (Micromeritics, USA). Electrochemical impedance spectroscopy (EIS) was conducted using a Par 2273 Potentiostats-Electrochemistry Workstation in 5 mM $Fe(CN)_6^{4-/3-}$ and 0.1 M KCl solutions at +0.25 V from 0.1 Hz to 10.0 KHz or in 0.5 M H_2SO_4 containing 0.5 M methanol at 0.676 V. The EIS data were fitted using ZSimpWin data analysis software. Cyclic voltammogram (CV) and chronoamperometry were performed using a CHI 660C electrochemical workstation. A three-electrode configuration was employed, with a modified glassy carbon (GC) electrode serving as the working electrode, and Ag/AgCl (in saturated KCl solution) and platinum wire serving as the reference and counter electrodes, respectively.

2.2. Preparation of HCSs and Pt/HCSs

The preparation of HCSs is presented in Scheme 1. Monodisperse SiO_2 spheres (2 g) were dispersed in 25 mL of methanol. After ultrasonication for 30 min, 2 mL of [VEIM]BF_4 were added to the methanol and 80 mg of AIBN was used as a polymerization initiator for the ILs monomers. The mixture was ultrasonicated for another 30 min and refluxed with vigorous stirring under an N_2 atmosphere for 12 h at 80 °C. The precipitate was collected by centrifugation and washed several times with acetone and double distilled water and then dried at 60 °C. The sample was carbonized in a tube furnace under a flow of N_2 at 900 °C for 3 h. The silica spheres were removed using an HF solution (10 wt%). The black product was washed with double distilled water and dried at 80 °C.

Either HCSs or Vulcan XC-72 (25 mg) were dispersed in 20 mL of double distilled water containing 22.5 mg of $H_2PtCl_6{\cdot}6H_2O$ before 2 mL of HCOOH was added dropwise with ultrasonication. The solution was stored at room temperature for 72 h, and the product was collected and dried at 60 °C. Approximately 60 min of ultrasonication was necessary to disperse 3 mg of Pt/HCSs or Pt/Vulcan XC-72 into a mixture of 0.1 mL (5 wt%) of Nafion and 0.9 mL of distilled water. The electrode was dried in air after 5 μL of the suspension was dropped onto the electrode surface.

3. Results and discussion

3.1. Characterization of HCSs and Pt/HCSs

Fig. 1a and b shows the SEM images of the SiO_2 particles, which possess a uniform size of 105 nm. Fig. 2a presents the SEM image of the as-prepared HCSs, which indicates that the HCSs consist of small adhesive spherical particles 120 nm in size. The energy-

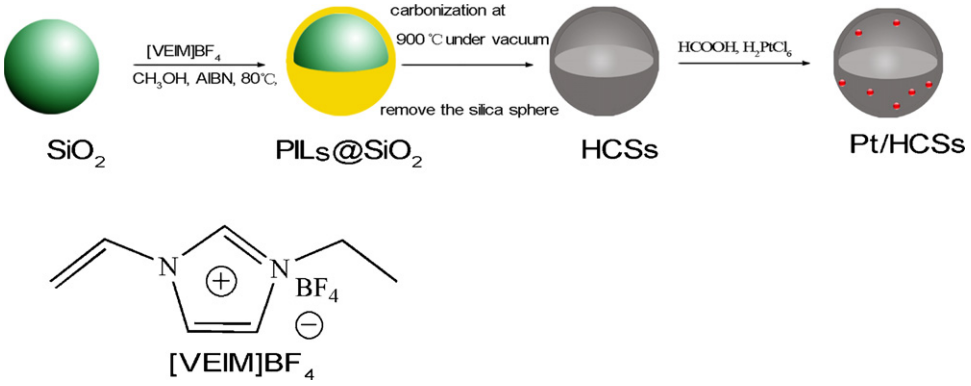

Scheme 1. Preparation pathway of the HCSs and Pt/HCSs nanocomposites.

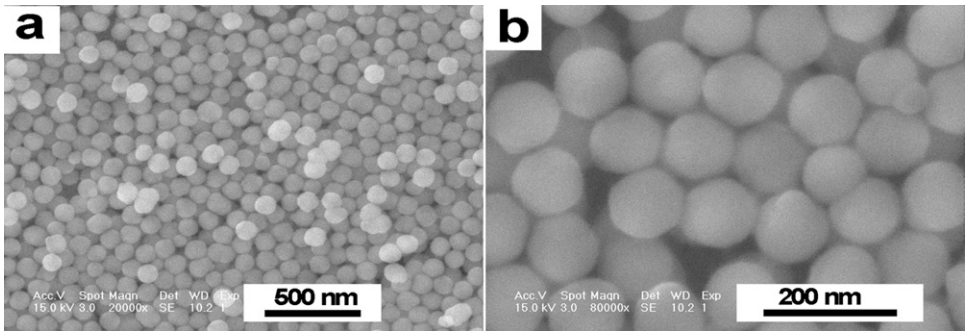

Fig. 1. (a) and (b) SEM images of the SiO_2 spheres.

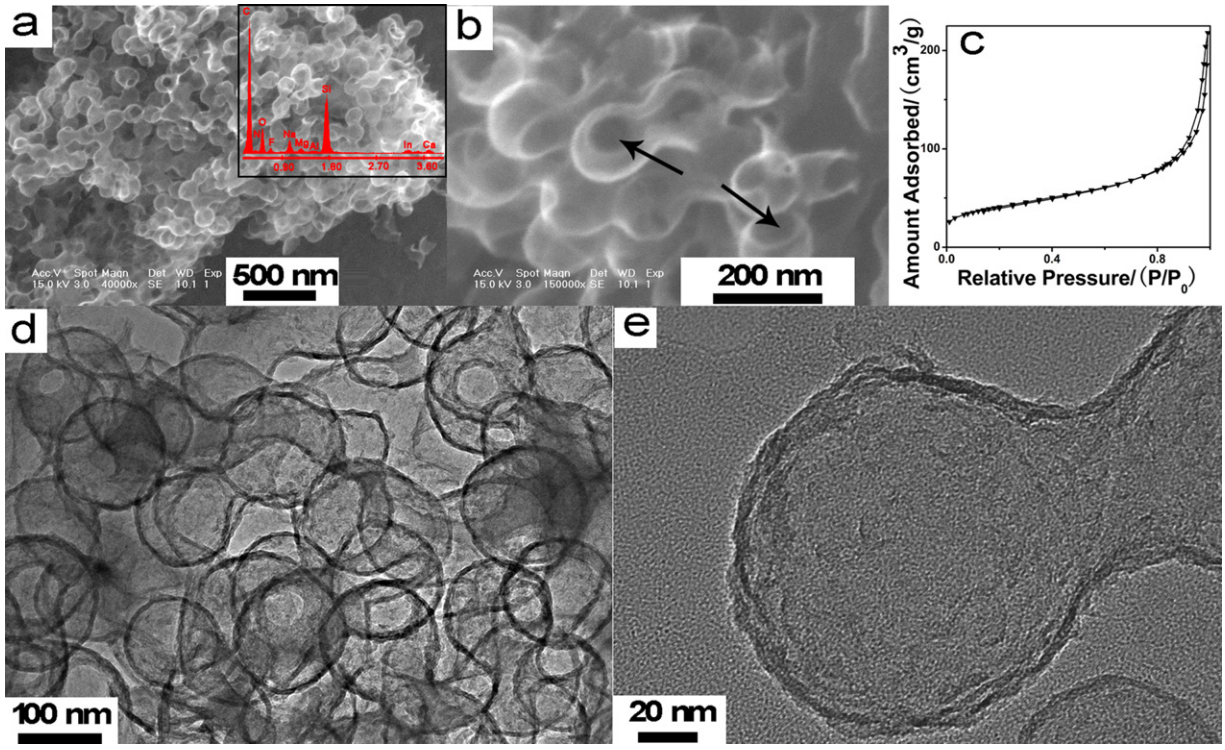

Fig. 2. (a) and (b) SEM images of the HCSs. (c) Nitrogen adsorption–desorption isotherm of the HCSs. (d) and (e) TEM images of the HCSs. Inset of (a) shows the EDX spectrum of the HCSs.

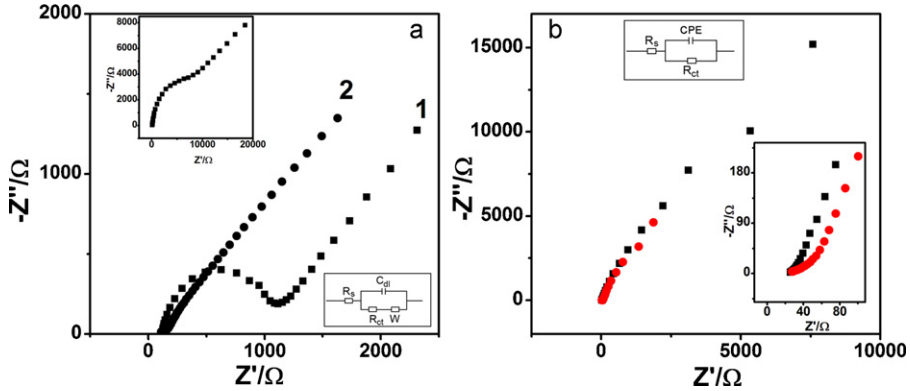

Fig. 3. (a) EIS results of (1) GC and (2) HCSs/Nafion/GC in a 0.10 M KCl solution containing 5 mM $Fe(CN)_6^{4-/3-}$ and at +0.25 V from 0.1 Hz to 10.0 KHz. Inset shows EIS of Nafion/GC in a 0.10 M KCl solution containing 5 mM $Fe(CN)_6^{4-/3-}$ at +0.25 V from 0.1 Hz to 10.0 KHz and the equivalent circuit. (b) EIS results of Pt/HCSs (black) and Pt/Vulcan XC-72 (red) in a 0.5 M H_2SO_4 solution containing 0.5 M methanol at 0.676 V from 0.1 Hz to 10.0 KHz. Inset shows the amplification of EIS of Pt/HCSs (black) and Pt/Vulcan XC-72 (red) and the equivalent circuit. (For interpretation of the references to color in this figure legend, the reader is referred to the web version of this article.)

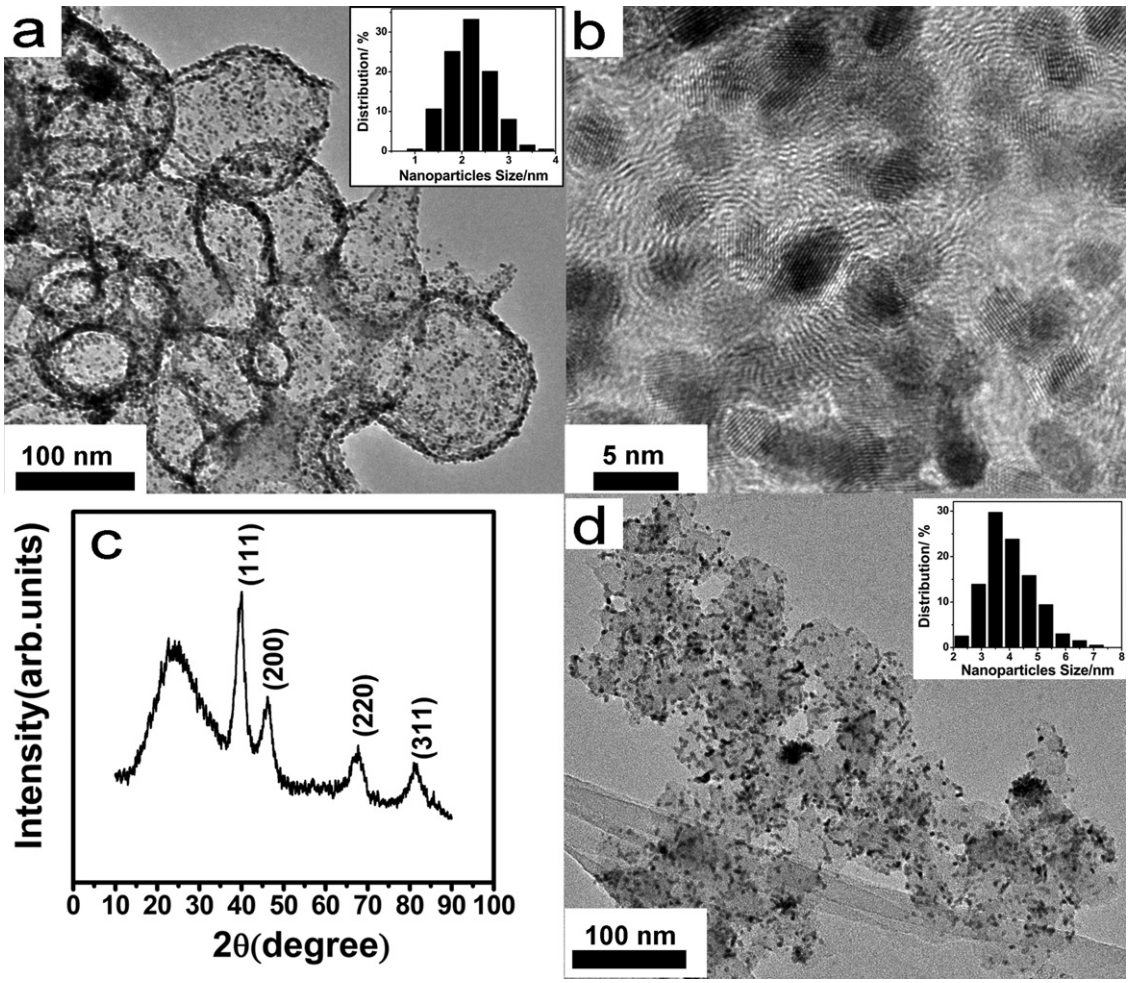

Fig. 4. (a) TEM image of Pt/HCSs. Inset indicates the particle size distribution of the Pt nanoparticles on the HCSs. (b) HRTEM image of the Pt/HCSs. (c) Wide-angle XRD of the Pt/HCSs nanocomposite. (d) TEM image of the Pt/Vulcan XC-72. Inset shows the particle size distribution of the Pt nanoparticles on Vulcan XC-72.

dispersive X-ray (EDX) spectrum was obtained to determine the composition of the HCSs. The EDX spectrum of the HCSs (inset of Fig. 2a) shows peaks corresponding to the elements C, N, and F (the other elements are derived from the ITO glass) and confirms the presence of N and F in the HCSs. The HCSs retain the morphology of the SiO_2 particles. Fig. 2b shows that some of the carbon spheres were partially open, indicating that they have a hollow structure (marked by the black arrow). This observation, obtained from SEM, indicates HCSs that are structurally robust replicas of the template can be fabricated successfully from PILs using the procedure shown in Scheme 1. Fig. 2c shows the nitrogen adsorption–desorption isotherm of the HCSs. A pronounced capillary condensation step is observed at the relative pressures between 0.8 and 1.0, which is assigned to the macropores generated by the removal of the SiO_2 sphere templates. The results show HCSs are mostly a macroporous material with an area of 142 $m^2\ g^{-1}$ and pore volume of 0.33 $cm^3\ g^{-1}$ according to BET. Fig. 2d and e shows the TEM images of the HCSs. Hollow sphere morphology with a core size of 105 nm and a shell thickness of 7 nm is observed in the carbonized sample. The size of the hollow core is consistent with the diameter of the SiO_2 template.

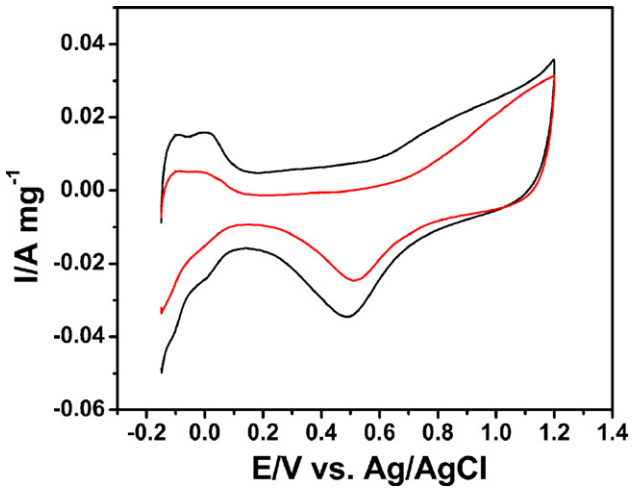

Fig. 5. CVs of Pt/HCSs (black line) and Pt/Vulcan XC-72 (red line) under an N_2 atmosphere 0.5 M H_2SO_4.

EIS was used to study the electron-transfer kinetics of the HCSs. Fig. 3a shows the EIS results from the three electrodes. Obviously, the bare GC electrode (1) exhibits a semicircle portion with a large diameter and an estimated value for R_{ct} of 561 Ω. After the GC was modified with a Nafion film (inset of Fig. 3a), the R_{ct} increased markedly and was calculated to be 2277 Ω, probably due to the Nafion film acting as a barrier and blocking the interfacial charge transfer. In contrast, HCSs (2) show a very low electron-transfer resistance (30 Ω) for the redox probe, suggesting that HCSs have a high electrical conductivity and improve the electron-transfer

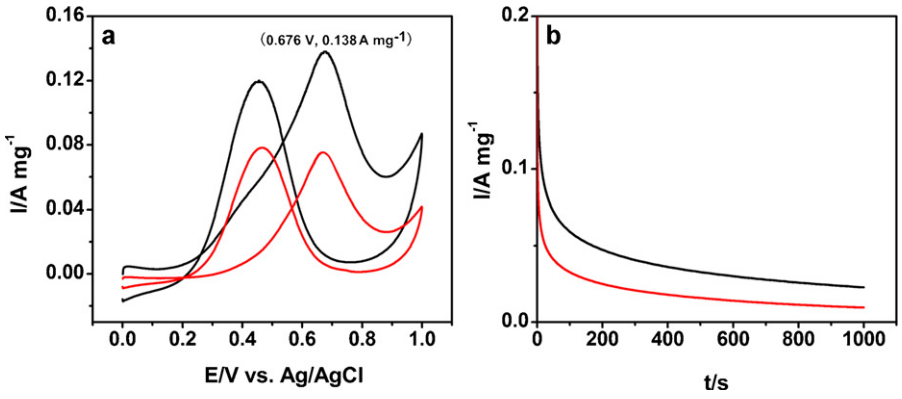

Fig. 6. (a) CVs of Pt/HCSs (black line) and Pt/Vulcan XC-72 (red line) in a 0.5 M H_2SO_4 solution with 0.5 M methanol at 50 mV s^{-1}. (b) Chronoamperometric results for the oxidation of methanol at 0.676 V on Pt/HCSs (black line) and Pt/Vulcan XC-72 (red line).

rate. EIS measurements were also performed to further evaluate the electron transfer kinetics for the oxidation of methanol on both the Pt/HCSs and Pt/Vulcan XC-72 electrocatalyst (Fig. 3b). The charge-transfer resistance of Pt/HCSs (black) is less than that of Pt/Vulcan XC-72 (red). This indicates the rate of oxidation of methanol using the Pt/HCSs catalyst was faster than for the Pt/Vulcan XC-72 catalyst, confirming the higher electrocatalytic activity of Pt/HCSs.

Fig. 4a shows the TEM image of the Pt/HCSs, which indicates that the spherical morphology is basically retained after the incorporation of the Pt nanoparticles. It can be seen that the Pt nanoparticles are uniformly dispersed onto the HCSs. The average diameter of 200 particles was found to be 2.8 nm, as shown in the histogram (inset of Fig. 4a). An HRTEM (Fig. 4b) confirms that the HCSs are successfully decorated with many well-dispersed Pt nanoparticles. The high surface area and unique structure facilitates the fine dispersion of the Pt nanoparticles. Several characteristic peaks for Pt are present in the wide-angle XRD spectrum of the Pt/HCSs nanocomposite, as shown in Fig. 4c. These peaks correspond to the planes (1 1 1), (2 0 0), (2 2 0), and (3 1 1) at 2θ of around 39.7°, 46.1°, 67.7°, and 81.5°, respectively, and confirm the formation of a Pt/HCSs nanocomposite. Pt nanoparticles supported on Vulcan XC-72 exhibit large particle sizes (Fig. 4d) between 2 and 8 nm (inset of Fig. 4d) with a mean size of 4.0 nm.

The Pt/HCSs and Pt/Vulcan XC-72 electrodes were characterized electrochemically in N_2-saturated 0.5 M H_2SO_4 solution at 50 mV s^{-1} (Fig. 5). The electrochemical surface area (ESA) of the Pt nanoparticles supported on the HCSs and Vulcan XC-72 can be estimated by measuring the charge using the hydrogen electroadsorption curves (Q_H) according to the following equation:

$$\mathrm{ESA} = \frac{Q_H}{Q_{ref} \times \text{Pt loading}}$$

Q_H represents the charge of hydrogen adsorption/desorption and Q_{ref} = 0.21 mC cm^{-2}, representing the surface density of the polycrystalline Pt electrode, generally accepted to be 1.3×10^{15} Pt atoms per cm^2. The results show that the ESA of Pt/HCSs (76 m^2 g^{-1} Pt) is approximately 1.55 times larger than that of the Pt/Vulcan XC-72 (49 m^2 g^{-1} Pt).

3.2. Electrocatalytic oxidation of methanol

The catalytic activity of the Pt/HCSs towards the oxidation of methanol was investigated. Fig. 6a presents the CVs of Pt/HCSs (black line) and Pt/Vulcan XC-72 (red line) in 0.5 M H_2SO_4 in the presence of 0.5 M methanol at 50 mV s^{-1}. A significant enhancement to the peak current and an obvious negative shift of the onset potential can be observed for Pt/HCSs relative to Pt/Vulcan XC-72. The maximum peak value of oxidation current density on Pt/HCSs is 0.138 A mg^{-1}, whereas that for Pt/Vulcan XC-72 is 0.075 A mg^{-1}. This value is also higher than those for Pt on HCSs derived from glucose (0.046 A mg^{-1} for 0.5 M methanol at 50 mV s^{-1}) [23] and Pt/Sn/CNTs (0.091 A mg^{-1} for 1 M methanol at 50 mV s^{-1}) [24]. Although the high catalytic activity of Pt/HCSs when compared to other carbon sources partly compensates for the high price of ILs, further investigation is needed to alleviate the high cost of this synthetic method. The ratio of the forward oxidation (I_f) to the reverse oxidation (I_b), I_f/I_b, can be used to evaluate the tolerance of the catalysts to poisoning. High I_f/I_b ratio indicates more effective removal of any poisoning species from the catalysts' surface. The I_f/I_b ratio of Pt/HCSs is 1.16. This value is higher than that of the Pt/Vulcan XC-72 (0.96), which demonstrates better tolerance than Pt/Vulcan XC-72. The higher current density for the oxidation of methanol using HCSs was further confirmed by chronoamperometric measurements performed at +0.676 V (Fig. 6b). Electro-oxidation of methanol on Pt/HCSs nanocomposites possesses a higher initial current and limiting current density. The current density for Pt/HCSs (black line) at 1000s is 2.38 times greater than that of the Pt/Vulcan XC-72 catalyst (red line) for the oxidation of methanol. The above electrocatalytic data reveals that Pt supported on HCSs exhibits higher activity than Vulcan XC-72 for the oxidation of methanol. The unique structure and high surface area of the HCSs allow the formation of highly dispersed Pt nanoparticles. The smaller Pt nanoparticles then enable the improved electrocatalytic activity observed for Pt/HCSs.

4. Conclusion

In summary, HCSs were prepared using PILs as a carbon precursor and monodisperse silica particles as a template for the first time. The obtained HCSs possessed a hollow sphere morphology with a core size of 105 nm and a shell thickness of 7 nm. The size of the hollow core is consistent with the diameter of SiO_2 template. A high surface area and suitable porosity makes HCSs a suitable support for Pt electrocatalysts. The hollow, porous structure of the HCSs results in more efficient mass transport, while the high surface area of HCSs allows for a greater dispersion of the Pt nanoparticles. Compared to the Pt/Vulcan XC-72 catalyst, the Pt/HCSs catalyst displays a high activity towards the oxidation of methanol.

Acknowledgements

The authors gratefully acknowledge the financial support of the National Natural Science Foundation of China (21075014) and the Fundamental Research Funds for the Central Universities (No. 10SSXT141).

References

[1] E.A. Franceschini, G.A. Planes, F.J. Williams, G.J.A.A. Soler-Illia, H.R. Corti, J. Power Sources 196 (2011) 1723–1729.
[2] M. Soszko, M. Lukaszewski, Z. Mianowska, A. Czerwinski, J. Power Sources 196 (2011) 3513–3522.
[3] D. Xu, Z. Liu, H. Yang, Q. Liu, J. Zhang, J. Fang, S. Zou, K. Sun, Angew. Chem. Int. Ed. 48 (2009) 4217–4221.
[4] Z.L. Schaefer, M.L. Gross, M.A. Hickner, R.E. Schaak, Angew. Chem. Int. Ed. 49 (2010) 7045–7048.
[5] S.J. Teng, X.X. Wang, B.Y. Xia, J.N. Wang, J. Power Sources 195 (2010) 1065–1070.
[6] J.J. Niu, J.N. Wang, J. Mater. Chem. 18 (2008) 5921–5926.
[7] J.H. Kim, J.S. Yu, Phys. Chem. Chem. Phys. 12 (2010) 15301–15308.
[8] J. Fu, Q. Xu, J. Chen, Z. Chen, X. Huang, X. Tang, Chem. Commun. 46 (2010) 6563–6565.
[9] L. Guo, L. Zhang, J. Zhang, J. Zhou, Q. He, S. Zeng, X. Cui, J. Shi, Chem. Commun. (2009) 6071–6073.
[10] R.J. White, K. Tauer, M. Antonietti, M.-M. Titirici, J. Am. Chem. Soc. 132 (2010) 17360–17363.
[11] B. Wu, D. Hu, Y. Kuang, B. Liu, X. Zhang, J. Chen, Angew. Chem. Int. Ed. 48 (2009) 4751–4754.
[12] Y. Liu, D. Wang, J. Huang, H. Hou, T. You, Electrochem. Commun. 12 (2010) 1108–1111.
[13] D.-J. Guo, J. Power Sources 195 (2010) 7234–7237.
[14] G.B. Appetecchi, G.T. Kim, M. Montanino, M. Carewska, R. Marcilla, D. Mecerreyes, I. De Meatza, J. Power Sources 195 (2010) 3668–3675.
[15] J.S. Lee, X. Wang, H. Luo, G.A. Baker, S. Dai, J. Am. Chem. Soc. 131 (2009) 4596–4597.
[16] J.S. Lee, X. Wang, H. Luo, S. Dai, Adv. Mater. 22 (2010) 1004–1007.
[17] X. Wang, S. Dai, Angew. Chem. Int. Ed. 49 (2010) 6664–6668.
[18] W. Yang, T.-P. Fellinger, M. Antonietti, J. Am. Chem. Soc. 133 (2010) 206–209.
[19] B.J.P. Paraknowitsch, J. Zhang, D. Su, A. Thomas, M. Antonietti, Adv. Mater. 22 (2010) 87–92.
[20] J. Yuan, C. Giordano, M. Antonietti, Chem. Mater. 22 (2010) 5003–5012.
[21] M. Antonietti, D. Kuang, B. Smarsly, Y. Zhou, Angew. Chem. Int. Ed. 43 (2004) 4988–4992.
[22] W. Stöber, A. Fink, E. Bohn, J. Colloid Interface Sci. 26 (1968) 62–69.
[23] Z. Wen, Q. Wang, Q. Zhang, J. Li, Electrochem. Commun. 9 (2007) 1867–1872.
[24] S. Sun, G. Zhang, D. Geng, Y. Chen, M.N. Banis, R. Li, M. Cai, X. Sun, Chem. Eur. J. 16 (2010) 829–835.